INTERACTION NOTE

Note 156

INTEGRAL EQUATION SOLUTION AND RCS COMPUTATION OF A THIN RECTANGULAR PLATE

December 1973

Y. Rahmat-Samii and R. Mittra
Department of Electrical Engineering
University of Illinois
Urbana, Illinois 61801

ABSTRACT

In this work a new integral equation is employed to calculate the current distribution on a rectangular plate which is illuminated by a plane wave. Numerical results are also obtained for the radar cross section of the plate for different angles of incidence and different dimensions of the plate. These results are compared with other RCS computations using GTD, physical optics and variational methods.

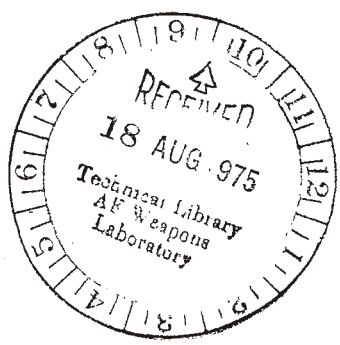

INTRODUCTION AND FORMULATION

In a recent paper [1] the authors have examined the question of the failure of the H-integral equation for thin, planar structures, and have derived a new integral equation by manipulating the E- and H-integral equations. The purpose of this note is twofold: to present a direct method for deriving the above-mentioned equation and transform it to an alternative form which is preferable for numerical computation; to compute the current distribution and RCS of a thin plate and compare the RCS results with other methods.

Let a plane electromagnetic wave with arbitrary polarization be incident upon a thin perfectly conducting rectangular plate of dimensions a and b. Assuming the $e^{j\omega t}$ time convention, the incident wave may be written:

$$\vec{H}^i = \left(H^i_{0x}\hat{x} + H^i_{0y}\hat{y} + H^i_{0z}\hat{z}\right) e^{j(k_x x + k_y y + k_z z)} \tag{1}$$

where $k_x = k \sin\theta \cos\phi$, $k_y = k \sin\theta \sin\phi$, $k_z = k \cos\theta$, $k = 2\pi/\lambda$, and θ and ϕ are the elevation and azimuthal angles of incidence, respectively.

Let us denote the induced current on the structure by $\vec{J}\delta(z)$ and the vector potential by $\vec{A}$. Expressing the scattered E-tangential field in terms of $\vec{J}$ and $\vec{A}$, and applying the boundary condition on the plate, viz., $\vec{E}_{Scatt} = -\vec{E}^i$, we obtain

$$\nabla \times \nabla \times \vec{A} - \vec{J}\delta(z) = -\nabla \times \vec{H}^i \ . \tag{2}$$

Similarly, requiring that the total normal -H on the plate to be zero leads to the equation:

$$\hat{z} \cdot (\nabla \times \vec{A} + \vec{H}^i) = 0 \ . \tag{3}$$

As a first step toward deriving the desired integral equation we substitute the tangential (x and y) derivatives of (3) into (2) to obtain

$$\frac{\partial^2}{\partial x^2} + \frac{\partial^2}{\partial y^2} + k^2 \iint_s \vec{J}\Phi \, dx' \, dy' = -\hat{z} \times \frac{\partial \vec{H}^i}{\partial z} \ , \quad \{z = 0;\ 0 < x < a,\ \ 0 < y < b\} \tag{4}$$

where $\Phi = (4\pi)^{-1} \exp\{-jk|\vec{r} - \vec{r}'|\}/|\vec{r} - \vec{r}'|$. In deriving (4), $\vec{A}$ has been replaced by $\iint_s \vec{J}\Phi \, dx' \, dy'$ and the defining equation for $\vec{A}$, viz., $(\nabla^2 + k^2)\vec{A} = -\vec{J}\delta(z)$, has been used. The same type of integro-differential equation has also been derived by Van Bladel [2] following Bouwkamp's method [3] for an aperture in an infinite screen.

It should be noted that, as indicated above, the range of validity of (4) is strictly restricted to $0 < x < a$ and $0 < y < b$. Specifically, the above equation is not complete at the edges of the plate, i.e., $x = 0$, a and $y = 0$, b. If (4) were to represent a complete description of the problem, it would have implied that the two current components J_x and J_y are indeed uncoupled with respect to the incident polarization. It is well-known that this situation is true for an infinite planar structure only and that two components of the current are always coupled in a finite structure. This coupling phenomenon becomes evident, however, when (4) is transformed into an alternate form, shown below, and when appropriate boundary conditions are imposed on J_x and J_y at the rim of the plate. Incidentally, (4) is not valid at the rim because the tangential derivative of the l.h.s. of (3) is meaningful only when the rim is excluded.

The alternate equation is derived by integrating the differential operator $(\partial^2/\partial x^2 + \partial^2/\partial y^2 + k^2)$ in the l.h.s. of (4) in an extended domain which leads to

$$\iint_s \vec{J}\Phi \, dx' \, dy' = \frac{-1}{jk_z} \{\hat{z} \times H_0^i\} e^{j(k_x x + k_y y)} + \frac{1}{k} \int_0^{2\pi} [\hat{x}C_1(\xi) + \hat{y}C_2(\xi)] e^{jk(x\cos\xi + y\sin\xi)} \, d\xi,$$

$$\{z = 0, \ 0 \leq x \leq a, \ 0 \leq y \leq b\} \qquad (5)$$

where $C_1(\xi)$ and $C_2(\xi)$ are two arbitrary functions. We note that the second term in the l.h.s. of (5) is a homogeneous solution to the two-dimensional Helmholtz operator $(\partial^2/\partial x^2 + \partial^2/\partial y^2 + k^2)$. It has been pointed out [1] that the inclusion of the homogeneous solution is necessary to obtain a complete

solution for the finite plate problem. Another point to note is that the limit of integration of the homogeneous term in (5) is chosen to be from 0 to 2π, which obviously corresponds to the visible range of the spectral angle ξ. By considering the asymptotic low frequency limit of the problem, the authors have shown [4] that this is the appropriate range of the integral in question.

Since (5) is also required to satisfy the boundary condition (3), i.e., $H_{normal} = 0$ on the plate, one can relate C_1 and C_2 as

$$\hat{x}C_1(\xi) + \hat{y}C_2(\xi) = (\hat{x}\cos\xi + \hat{y}\sin\xi)C(\xi) \tag{6}$$

where $C(\xi)$ is a known function yet to be determined.

An even more desirable form of (5) may be obtained by representing $C(\xi)$ in a Fourier series as

$$C(\xi) = \sum_{-\infty}^{\infty} C_n e^{jn\xi} \tag{7}$$

Using (6) and (7) in (5) and employing the well-known representation for Bessel's function, viz.,

$$J_n(k\rho) = \frac{j^n}{2\pi}\int_0^{2\pi} e^{-jk\rho\cos\beta} e^{jn\beta}\, d\beta \quad , \tag{8}$$

we obtain

$$\iint_s \begin{Bmatrix} J_x \\ J_y \end{Bmatrix} \Phi\, dx'\, dy' = \frac{1}{jk_z}\begin{Bmatrix} H^i_{0y} \\ -H^i_{0x} \end{Bmatrix} e^{j(k_x x + k_y y)} + \frac{\pi}{k}\begin{Bmatrix} 1 \\ -j \end{Bmatrix}\sum_{-\infty}^{\infty} C_n \left[j^{n+1} e^{j(n+1)\phi} J_{n+1}(k\rho) + \begin{Bmatrix} 1 \\ -1 \end{Bmatrix} j^{n-1} e^{j(n-1)\phi} J_{n-1}(k\rho) \right] \tag{9}$$

where (ρ,ϕ) are the polar coordinates of the point (x,y).

The unknown currents J_x and J_y can now be obtained by solving (9) in conjunction with the auxiliary condition $\vec{J}\cdot\hat{\nu} = 0$, where $\hat{\nu}$ is a unit normal to the edge of the plate. Note that in contrast to the E-integral equation there are no differential operators in the kernel of (9) which makes it rather

convenient for numerical processing. In fact, the moment method [5] may be used to solve (9) with accuracy using simple pulse functions for basis and δ functions for weights. Applying the moment method as indicated, (9) is transformed into a discretized form:

$$\sum_{m=1}^{M}\sum_{n=1}^{N}\begin{Bmatrix} J_x(x'_m,y'_n) \\ J_y(x'_m,y'_n) \end{Bmatrix} \Phi(x_\ell,y_p;\, x'_m,y'_n)\Delta x\Delta y$$

$$= \frac{1}{jk_z}\begin{Bmatrix} H^i_{0y} \\ -H^i_{0x} \end{Bmatrix} e^{j(k_x x_\ell + k_y y_p)}$$

$$+ \frac{\pi}{k}\begin{Bmatrix} 1 \\ -j \end{Bmatrix} \sum_{n=1}^{L}\left\{ C_n\, j^{n+1}\, e^{j(n+1)\phi}\, J_{n+1}(k\rho) + \begin{Bmatrix} 1 \\ -1 \end{Bmatrix} j^{n-1}\, e^{j(n-1)\phi}\, J_{n-1}(k\rho)\right\} \tag{10}$$

$$\ell = 1, \ldots, M;\ p = 1, \ldots, N$$

where $\rho = \left(x_\ell^2 + y_p^2\right)^{1/2}$, $\phi = \arctan\,(y_p/x_\ell)$, and L, the upper limit in the summation in the r.h.s. of (10) corresponds to the total number of matching points on the rim. This is done in anticipation of the application of the boundary condition $\vec{J} \cdot \hat{\nu} = 0$, which is eventually used to determine the unknown C_n's.

The far field scattered by the plate may be readily computed once the current distribution on the plate has been determined from the solution of (10). The radar cross section (RCS) may then be computed by using the definition [6]:

$$\sigma = \lim_{r\to\infty} 4\pi\, r^2\, \frac{W_r}{W_i} \tag{11}$$

where W_r is the scattered power flux density at a distance r from the scatterer and W_i is the power flux density in an incident plane-wave field.

NUMERICAL RESULTS AND DISCUSSIONS

A general program has been written for the IBM 360/75 system that computes the current distribution and radar cross section for an arbitrary incident angle, arbitrary polarization, and arbitrary dimensions of the plate. Figures 1 and 2 show the distribution of the two components of the current sampled along the

principal axes, for an obliquely incident plane wave with E_y polarization. Note that the two components of the current exhibit correct behaviors at the edge of the plate, and that they are significantly different from the results given by the physical optics approximation.

In the process of analyzing the numerical behavior of (10), it has been found that this matrix equation gives better approximation to (5) than the form used in our earlier paper [1]. Also, it has been noticed that even when the condition $\vec{J} \cdot \hat{\nu} = 0$ is applied at only a fraction of subsections around the rim, this condition is satisfied at the in-between points as long as the separation between the match points is not too large. Furthermore, this separation distance can be estimated from the behavior at two neighboring match points of the highest order Bessel's function appearing in (10). The behavior of the solution is shown pictorially in the three-dimensional plots of Figures 3 and 4. Figure 3 shows the J_y component of the current distribution due to a normal incident field only prior to the incorporation of the contributions of the homogeneous terms in (10). It is obvious that by itself this current distribution does not have the correct behavior at the rim since it exhibits a singular behavior all around the rim. This was to be expected, however, since the solution of (5) is not complete without the homogeneous terms. Using the homogeneous terms and requiring that the normal component of the current goes to zero at the center of the dashed regions as indicated in Figure 4, one obtains the current distribution as shown in the same figure. It is seen that the current distribution now has the correct behavior around the entire rim, even though the condition $\vec{J} \cdot \hat{\nu} = 0$ has been imposed at only a third of the subsections around the edge. It may be of interest to mention that the above numerical results have been obtained with a matrix size of 81 x 81 for the 1λ square plate; however, no substantial loss of accuracy results if the size is reduced to 36 x 36.

Figure 5 shows the RCS vs. the angle of incidence for a 1λ x 1λ plate illuminated with an E_y^i-polarized plane wave. We have compared the present results with those derived by using the physical optics approximation (PO) and and the geometrical theory of diffraction (GTD). For this comparison we have used the formulations given by Ross [7] and have plotted the results of these computations in Figure 5. For angles of incidence less than 20° from the normal, all three methods are seen to be in good agreement. Even better agreement could have been obtained by imposing the boundary condition $\vec{J} \cdot \hat{v} = 0$ at precisely the physical edge of the plate rather than at the center of the edge sections. For angles of incidence between 20° and 65°, we observe that our results are in much better agreement with the GTD than with those obtained by using the physical optics approach. For angles greater than 80°, the results computed from the GTD formula given by Ross [7] appear to become increasingly inaccurate; however, the results obtained via the present approach appear to be good for the entire angular range.

Figure 6 shows the plots of RCS computations of a square plate for normal incidence and different plate sizes and a comparison of these curves with the corresponding ones reported in the RCS Handbook [8]. In this figure, the solid curve has been computed via the present formulation; circles indicate the experimentally measured data [8]; and the dashed curve has been obtained by applying the variational technique [8]. It is evident that our results exhibit a closer agreement with experimental data than those computed via the variational approach.

Finally, the complementary problem, that of coupling through an aperture in an infinite screen, has also been investigated [9] successfully using this approach, both with and without a back plate. It may also be worthwhile to mention that the decoupling of the E-equation is currently under study for cylindrical structures and the outlook appears to be quite promising.

ACKNOWLEDGEMENT

The authors would like to acknowledge the support from the U. S. Army Harry Diamond Laboratories and the Defense Nuclear Agency under Contract No. DAAG 39-73-C-0231, and the U. S. Army Research Office, Durham, North Carolina, Grant No. DA-ARO-D-31-124-71-G77.

REFERENCES

1. R. Mittra, Y. Rahmat-Samii, D. V. Jamnejad, and W. A. Davis, "A new look at the thin-plate scattering problem," Interaction Note 155, March 1973.

2. J. Van Bladel, Electromagnetic Fields. New York: McGraw-Hill Book Company, 1964, pp. 404-407.

3. C. J. Bouwkamp, "Diffraction theory," New York University, Mathematics Research Group, No. EM-50, 1953, p. 46.

4. R. Mittra and Y. Rahmat-Samii, "A systematic approach to the small hole coupling problem," (to appear).

5. R. E. Harrington, Field Computation by Moment Method. New York: Macmillan Company, 1968, pp. 82-89.

6. J. R. Mentzer, Scattering and Diffraction of Radio Waves. New York: Pergamon Press, 1955, pp. 2-10.

7. R. A. Ross, "Radar cross section of rectangular flat plates as a function of aspect angle," IEEE Trans. Antennas and Propagation, vol. AP-14, no. 3, pp. 329-335, May 1966.

8. C. T. Ruck, D. E. Barrik, W. D. Stuart, and C. K. Krichbaum, Radar Cross Section Handbook, ed., C. T. Ruck. New York: Plenum, 1970, p. 524.

9. Y. Rahmat-Samii and R. Mittra, "Electromagnetic coupling through apertures into a parallel-plate region," (to be published).

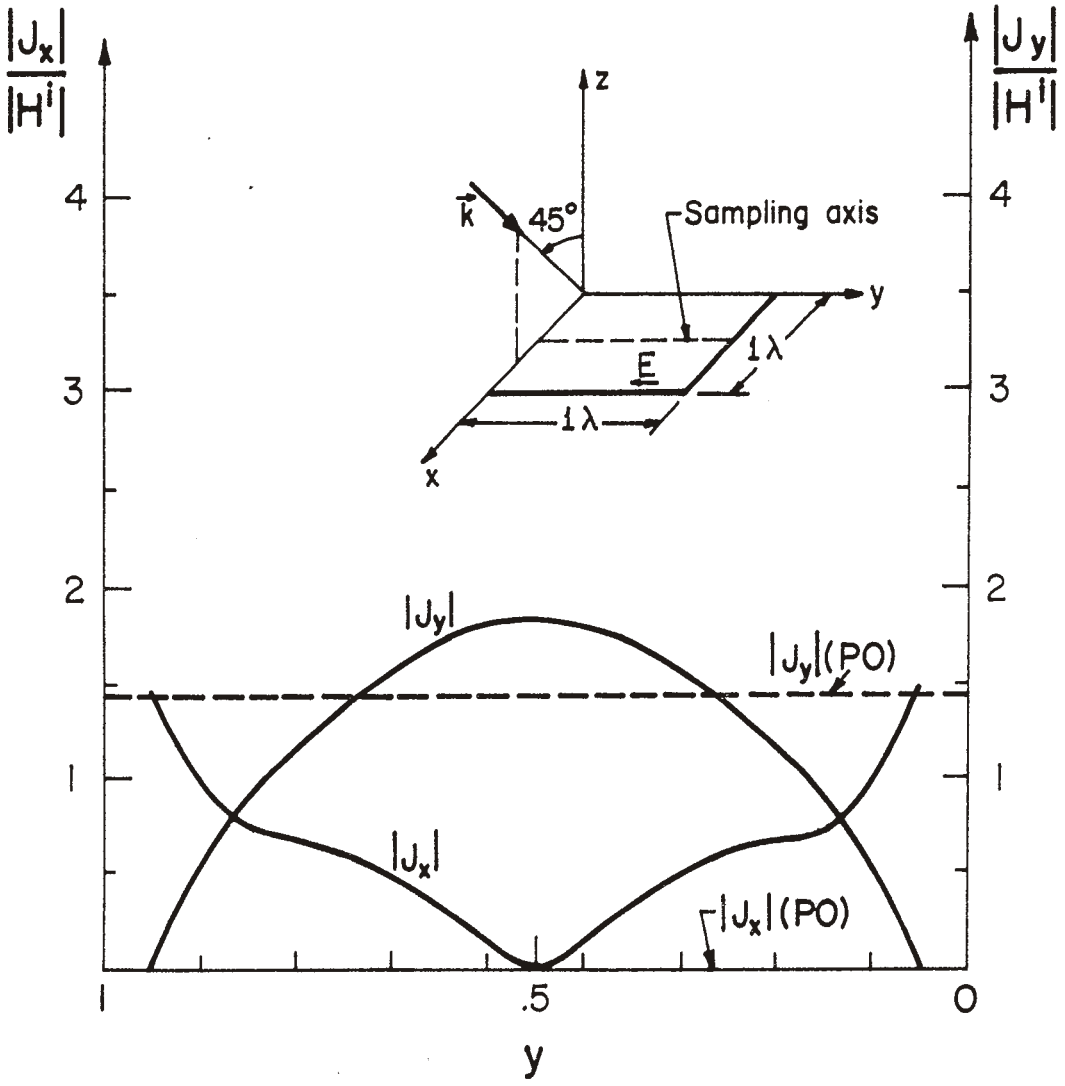

Figure 1. Amplitude of Current Distribution on a 1λ x 1λ plate.

x = λ/2 and y variable

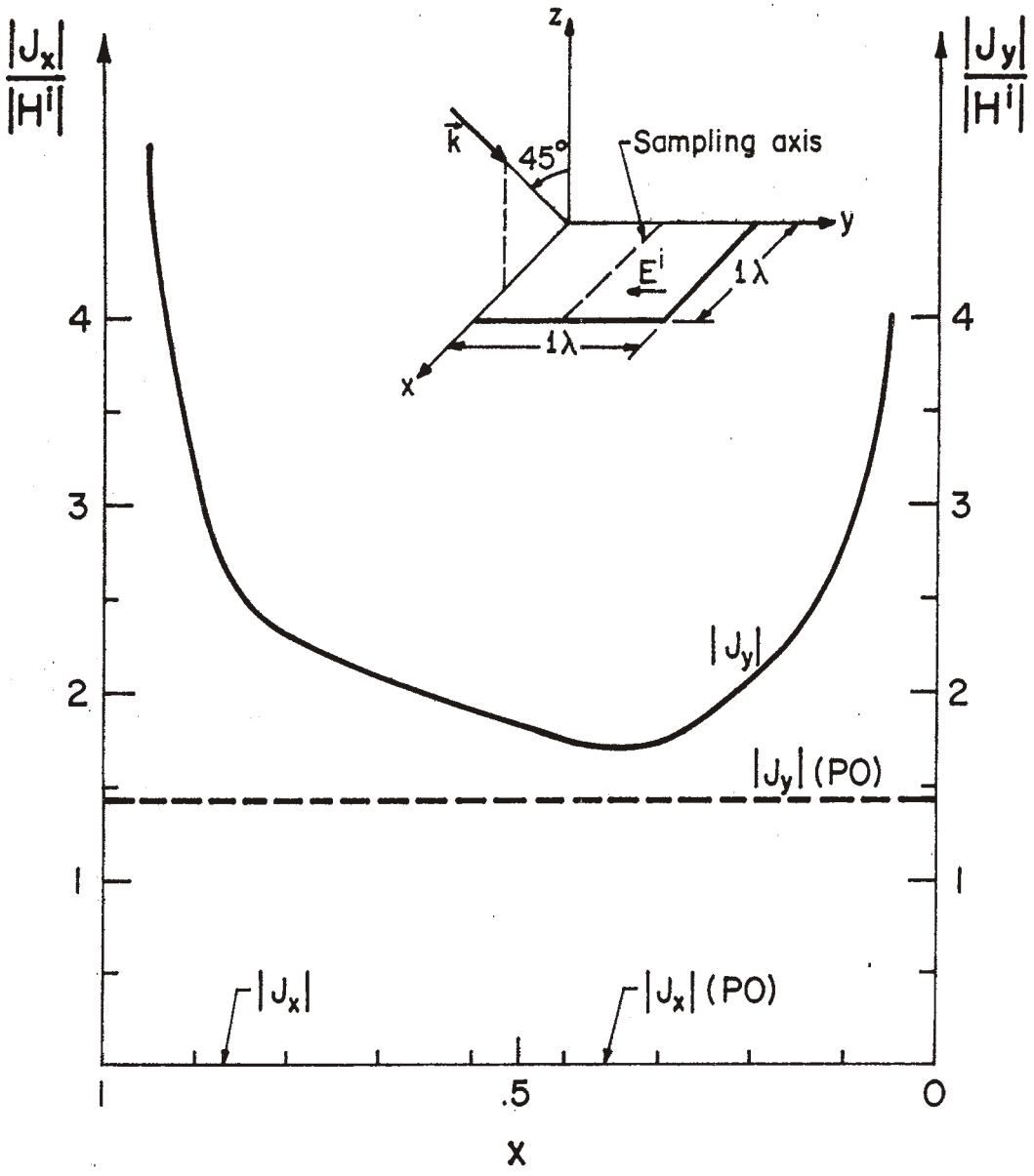

Figure 2. Amplitude of Current Distribution on a 1λ x 1λ Plate.

y = λ/2 and x variable

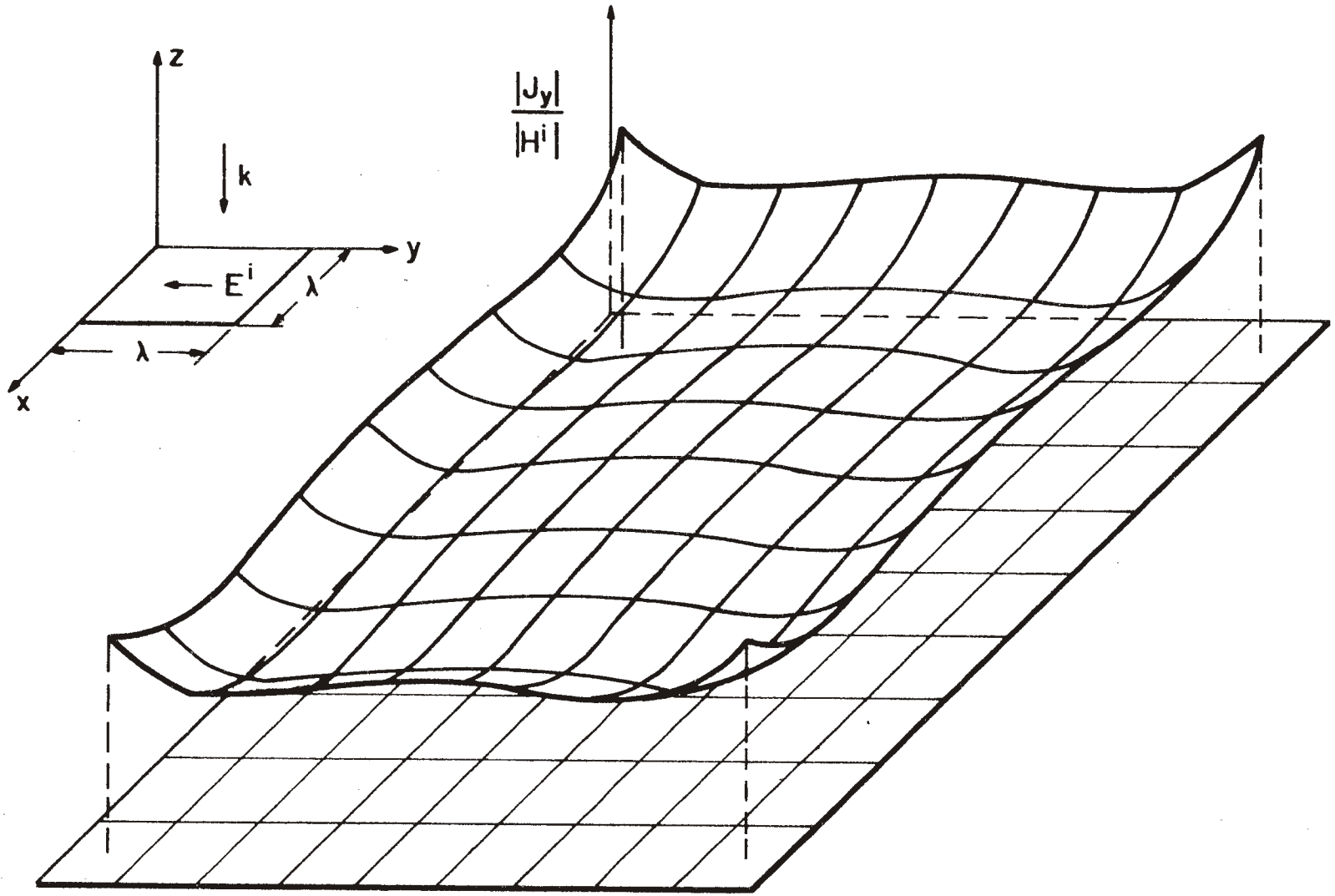

Figure 3. Amplitude of J_y Component of Current Distribution Computed from (10) Prior to Incorporating the Contribution of the Homogeneous Terms.

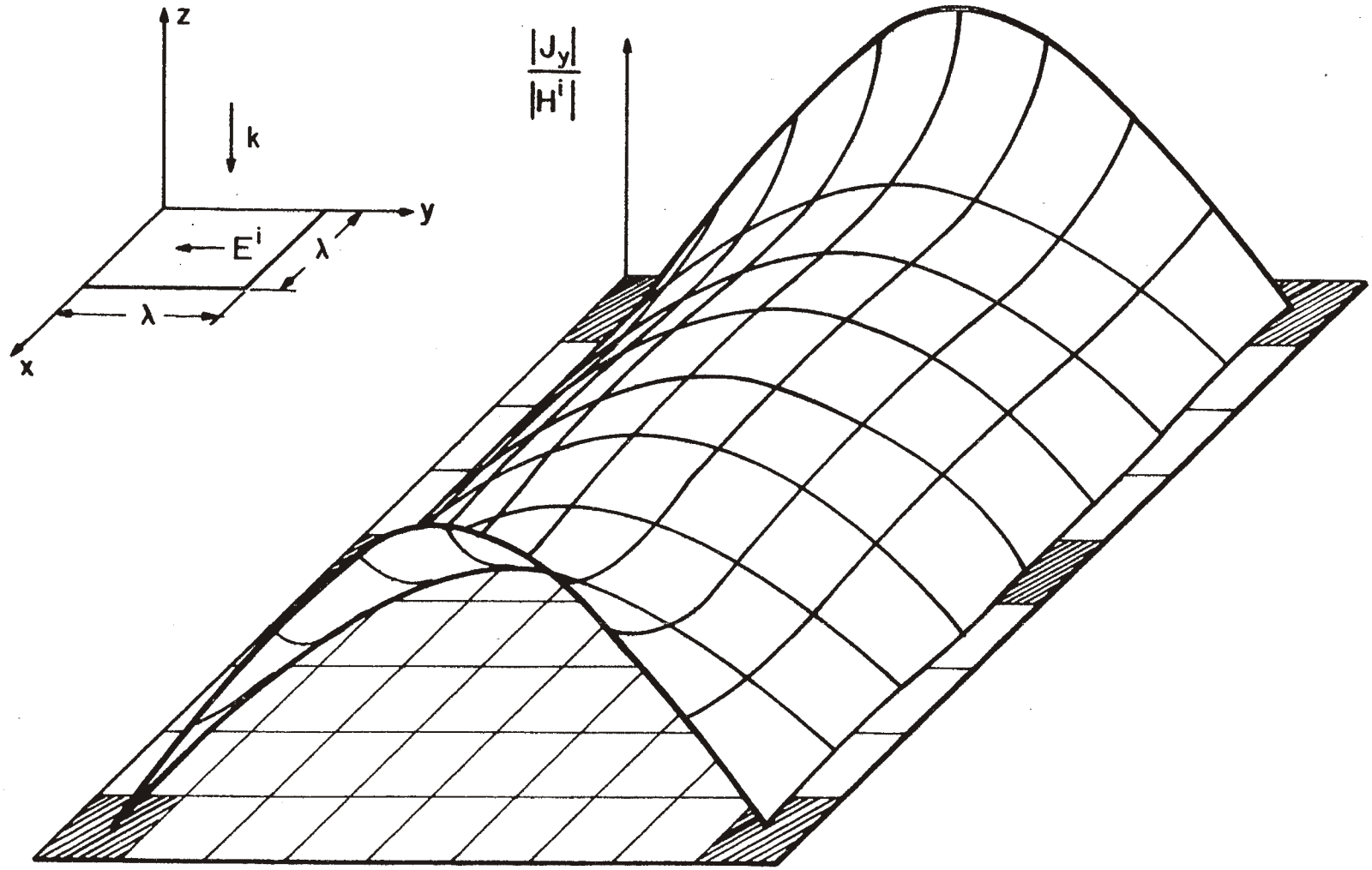

Figure 4. Amplitude of J_y Component of Current Distribution Obtained from (10) after Adding the Homogeneous Term Contributions.

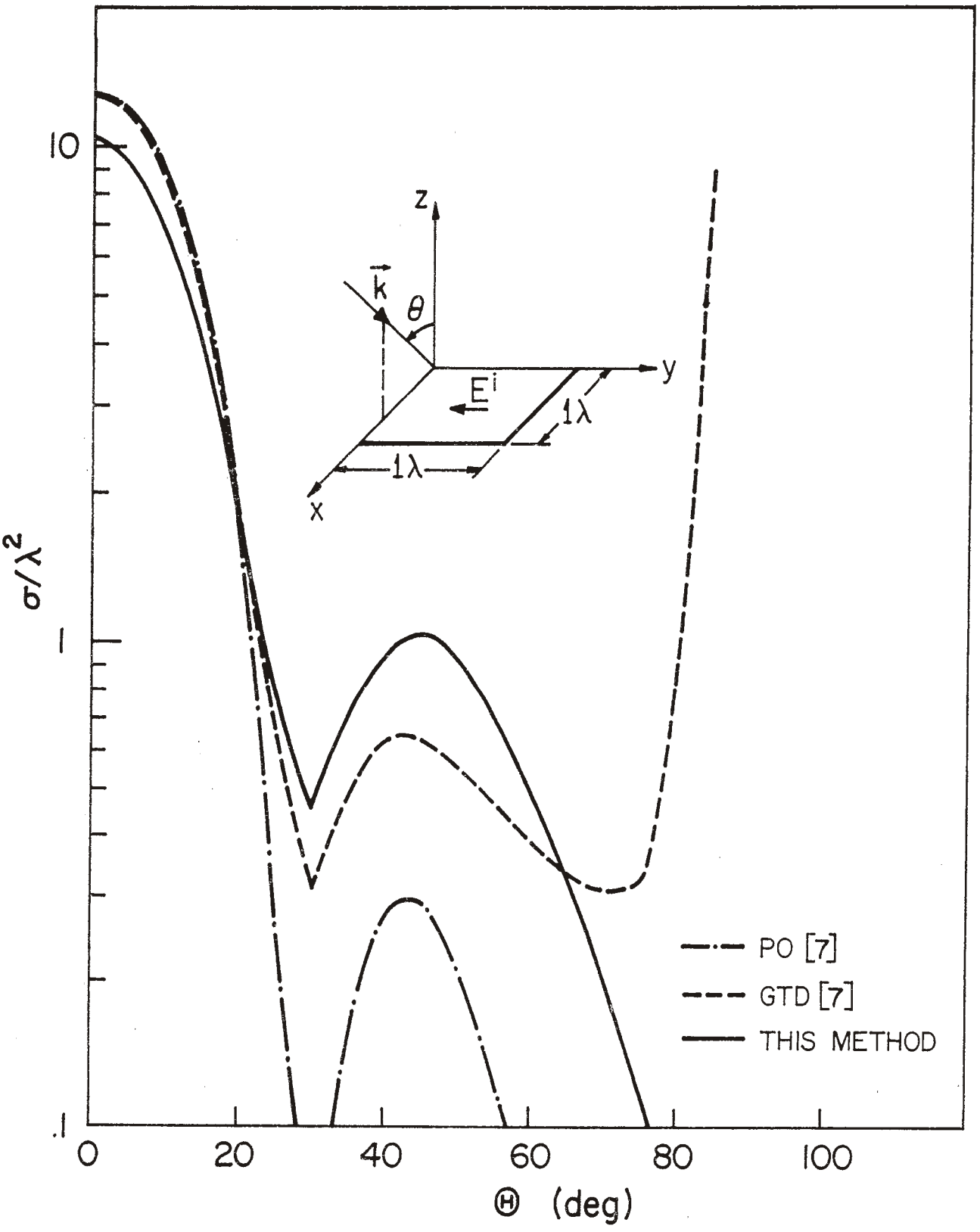

Figure 5. RCS of 1λ x 1λ Plate vs. Aspect Angle

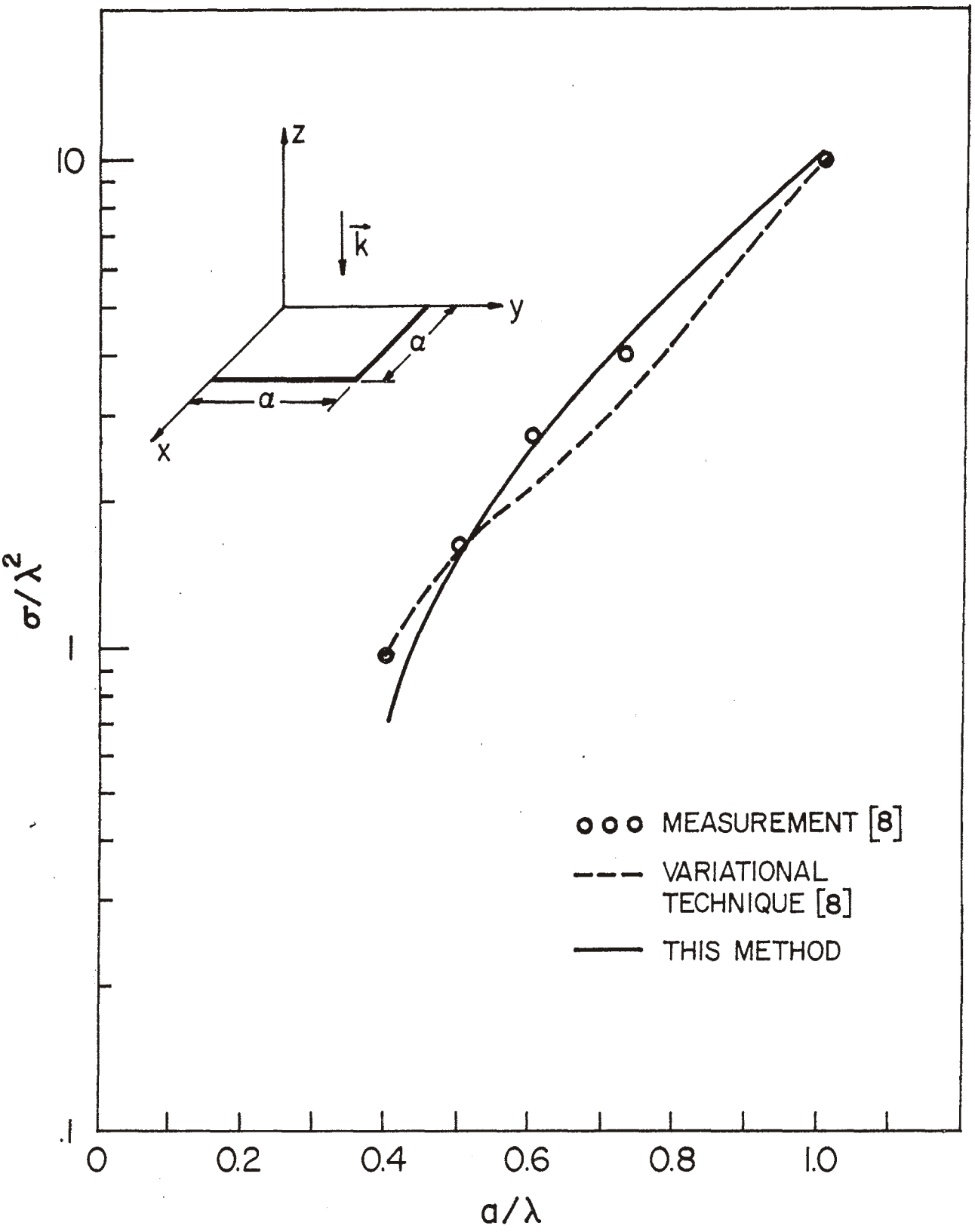

Figure 6. RCS of a Square Plate for Normally Incident Plane Wave.